Desalination and Water Treatment
www.deswater.com
doi: 10.1080/19443994.2015.1061954

57 (2016) 14067–14076
June

Taylor & Francis
Taylor & Francis Group

Effectiveness of a photocatalytic organic membrane for solar degradation of methylene blue pollutant

Ouassila Benhabiles[a,b], Hacene Mahmoudi[c,*], Hakim Lounici[a,d], Mattheus F.A. Goosen[e]

[a]*URIE. Ecole Nationale Polytechnique, Alger, Algérie, Tel./Fax: +213 24 41 04 84; email: benhabiles.ouassila@gmail.com (O. Benhabiles), Tel. +213 7 71 68 35 93; email: lounicih@yahoo.fr (H. Lounici)*
[b]*Unité de Développement des Equipements Solaires, UDES/Centre de Développement des Energies Renouvelables, CDER, BouIsmail 42415, W. Tipaza, Algérie*
[c]*Faculty of Technology, University Hassiba Benbouali of Chlef, Chlef, Algeria, Tel. +213 7 77170833; Fax: +213 27 727009; email: h.mahmoudi@univ-chlef.dz*
[d]*Faculty of Sciences, University of Bouira, Algeria*
[e]*Alfaisal University, Riyadh, Saudi Arabia, Tel. +966 53 2941468; email: mgoosen@alfaisa.edu*

Received 11 February 2015; Accepted 8 June 2015

ABSTRACT

The results of a feasibility study are presented on the use of a polystyrene (PS) organic membrane as a photocatalyst support in the degradation of organic pollutants in aqueous solution. Methylene blue (MB) was employed as a model dye and commercial titanium dioxide (TiO_2) was used as a photocatalyst. The MB dye which is resistant to direct photolysis especially at high concentrations was successfully eliminated by TiO_2 fixed on the PS membrane in aqueous dispersion under solar irradiation. Photodegradation results of MB showed that the film with 10 wt% TiO_2 exhibited a remarkable ultraviolet (sun light) photocatalytic activity over 5 h, with 68% of the pollutant being degraded. This is similar to a TiO_2 slurry system. The photocatalytic degradation obeyed pseudo-first-order kinetics at low initial MB concentration. The optimum pH for efficient removal of dye was found to be 11. An increase in initial dye concentration decreased the degradation rate. The applicability of Langmuir–Hinshelwood kinetic equation revealed that the degradation of MB occurred mainly on the surface of the photocatalyst. The concept and results provide a promising platform for fabricating highly efficient organic photocatalytic membranes for water treatment.

Keywords: Water treatment; Organic pollutant; Methylene blue; Solar photocatalysis; Immobilized TiO_2; Organic membrane

1. Introduction

Water pollution caused by organic chemicals produced from the textile, paper, plastic, leather, food, and mineral processing industries is a very serious problem [1,2]. This is mainly due to the presence of synthetic dyes that are resistant to bacterial degradation and conventional chemical processes. With the increasing shortage of clean water sources worldwide, the development of low-cost and efficient advanced water treatment technologies is urgently needed [1,2].

*Corresponding author.

There has been significant research on applying semiconductors for water treatment due to their effectiveness in degrading organic compounds [3,4]. A very promising technique for the separation of a catalyst from a reaction mixture at the end of a treatment process, for example, is to employ a fixed catalyst. Furthermore, photocatalytic treatments and membrane processes have also been increasingly applied to treat waste effluents from industry [1,2]. In particular, such catalysts have been widely used for the decomposition of harmful compounds in the environment [5–7]. Photocatalytic reactions allow for complete degradation of organic pollutants to small and in noxious species, without using chemicals, thus avoiding sludge production and disposal [5–7].

Titanium dioxide (TiO_2) which is a well-known semiconductor photocatalyst that has been applied in air purification, solar energy conversion, and wastewater treatment owes its success to its high photocatalytic activity, low cost, low photoerosion, non-toxicity, and excellent chemical and thermal stability under illumination [8–16]. In wastewater treatment processes, TiO_2 nanoparticles are generally used as a slurry system due to the large surface area of the catalysts, which affords high photocatalytic efficiency [17,18]. Nevertheless, the filtration to eliminate and recycle the powdered TiO_2 suspended in the treated water increases running cost and results in secondary pollution. This problem has become a limiting factor in practical application of the technology [19,20]. To avoid secondary pollution, much effort has been devoted to immobilizing TiO_2 on a variety of substrates [21], including glass [22,23], stainless steel [24], carbon fiber [25], titanium substrate [26,27], and polymers [28,29], by means of sol–gel method, thermal treatment, chemical vapor deposition (CVD), and electrophoretic deposition.

Membrane separation processes have been shown to be competitive with other separation processes in terms of energy costs, material recovery, being environmentally friendly, and being amenable to integrated processes for selective removal of impurities [30–33]. However, this technique only concentrates pollutants. It does not destroy the contaminants. What are needed are new technologies that reduce the use of chemicals in treatment processes thereby permitting a reduction in the global environmental impact. It can be argued that the coupling of a photocatalytic reaction with a membrane separation process could take advantage of the synergy of both technologies resulting in a very powerful system, with the membrane having the simultaneous task of supporting the photocatalyst as well as acting as a selective barrier for the species to be degraded [2,6,34,35].

Membrane separation may be combined with a photocatalysis process in what is called a photocatalytic membrane reactor (PMR). In such a reactor, the catalysts could be immobilized on the membrane surface or suspended in water [35,36]. Most of the previous work reported in the literature has focused on the use of TiO_2 photocatalysts suspended in water [37]. However, the problem with this system is that the photocatalyst has to be eventually separated from the suspension. A promising solution is to employ PMRs with TiO_2 photocatalysts immobilized on the membrane surface for wastewater treatment. The TiO_2 photocatalyst may be immobilized through physical absorption, hydrogen bonding, or chemical bonding.

Turchi and Ollis [38] reported on the TiO_2 photocatalysis reaction mechanisms. The initial photodegradation rates of different compounds were similar under identical conditions. This could only be explained by a rate-limiting step consisting of hydroxyl radical formation or attack. Since, adsorption is considered critical in the heterogeneous photocatalytic process, the Langmuir–Hinshelwood model was used to describe the photooxidation kinetics of dyes [39]. The Langmuir–Hinshelwood pseudo-first-order kinetic model modified to accommodate reactions occurring at a solid–liquid interface is as follows (1) [40]:

$$(r) = -\frac{\mathrm{d}C}{\mathrm{d}t} = \frac{kKC}{1+KC} = \frac{k_{\mathrm{app}}C}{1+kC+K_{\mathrm{s}}C_{\mathrm{s}}} \tag{1}$$

where r is the rate of degradation of the pollutant (mg/min); k is the reaction rate constant (mg/min); K the adsorption equilibrium constant of the reactant (L/mg); C the pollutant concentration (mg/L); k_{app} the apparent rate constant of degradation (min^{-1}); $K_{\mathrm{S}}C_{\mathrm{S}}$ the contribution of solvent.

Two cases are possible: for dilute solutions $KC \ll 1$:

$$(r) = -\frac{\mathrm{dc}}{\mathrm{d}t} = kKC = k_{\mathrm{app}}C \tag{2}$$

where k_{app} is the apparent rate constant of a reaction of pseudo-first-order. Eq. (2) can be integrated according to Eq. (3):

$$\ln\left(C_0/C\right) = k_{\mathrm{app}}t \tag{3}$$

The apparent rate constant k_{app} is determined from the slope of the curve obtained by representing $\ln(C/C_{\mathrm{o}})$ as a function of time t.

At high concentrations, Eq. (1) can be simplified and reduced to zero-order kinetics. Its integral form is given by Eq. (4):

$$(C_0 - C) = k_{app}t \quad (4)$$

The half-time reaction is very useful information for assessing the speed of a chemical reaction. It is determined from Eq. (3):

$$\text{for} \quad C = C_0/2 \qquad t_{1/2} = \ln(2)/k_{app} \quad (5)$$

The aim of the current study was to assess the effectiveness of a polystyrene (PS) organic membrane as a photocatalyst support in the degradation of organic pollutants in aqueous solution. Methylene blue (MB) was employed as a model dye and commercial TiO_2 was used as the photocatalyst under solar irradiation.

2. Experimental

2.1. Materials

In this study, PS used as a membrane material; it was a kind gift from the plastics industry in Algeria. The solvent used was acetone purchased from Chemical Factory "Biochem Chemo Pharma" (Quebec, Canada). Commercial TiO_2, photocatalyst used in our experiments was produced by the Chemical Factory "BiochemChemo Pharma" (Quebec, Canada).

The pollutant MB with chemical formula $C_{16}H_{18}ClN_3S$ is presented in Fig. 1. MB is an azoic dye widely used in the textile industry in Algeria, with the max absorption wavelength of 664 nm, provided by Biochem Chemopharma (Montreal, Quebec).

2.2. Membrane preparation

PS was dissolved in proper solvent to form 16 wt % casting solution at room temperature. The solvent was employed without further purification. A 4 wt% of a commercial form of inorganic photocatalytic TiO_2 was added to the casting solution under stirring. The solution was cast on a glass plate to a predetermined thickness of 40 μm with a Gardner knife. The glued membrane was then immersed in a coagulation bath (distilled water). After precipitation, the membranes were peeled off and dried in an oven at 60°C.

2.3. Membrane characterization and photocatalyst physical properties

The surface morphology and cross section of prepared TiO_2/PS composite membranes were observed using a scanning electron microscope SEM, Jeol JSM 630 SEM. The samples were coated with a thin sputtered gold layer under vacuum. Measurements of X-ray diffraction were performed using a PW 1729X-RAY GENERATOR PHILIPS device. This equipment uses Cu Kα1 radiation (λ = 1.5406 Å).

2.4. Solar photoreactor

The photocatalytic degradation of MB was carried out in a solar photoreactor located in northern Algeria (latitude 36°.39′; longitude 2°.42′ at sea level), during the period from August to September, using solar irradiation. The reactor was developed at the Solar Equipment Development Unit (SEDU) in Algeria. The effective volume of the photoreactor (32 cm

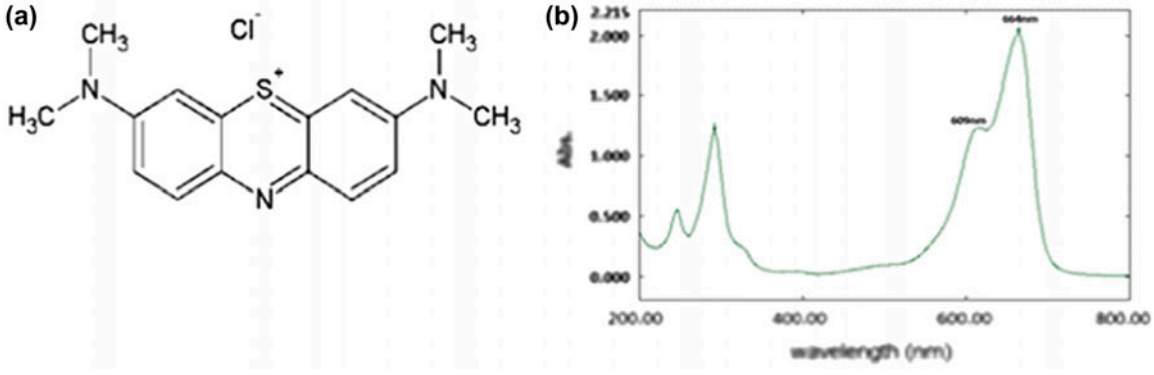

Fig. 1. (a) (LHS) Methylene blue (MB) chemical structure and (b) (RHS) UV–vis absorption spectrum of MB in aqueous solution.

length × 24 cm wide × 6.5 cm high) was 5 L. The photoreactor tank was made from Pyrex glass containing a flat membrane doped with 4 wt% catalyst as shown in Fig. 2.

During solar experiments, the intensity of solar radiation was measured with a Pyranometer CMP 11 (285–2,800 nm), which provides data in terms of incident W_{UV} m^{-2}. Thus, results could be referred to as accumulated UV energy, $Q_{UV,n}$ (kJ L^{-1}), calculated by Eq. (6) [41–43].

The quantity $Q_{UV,n}$ (kJ L^{-1}) is received on any surface in the same position with regards to the sun, per unit of volume of water inside the reactor, in the time interval Δt:

$$Q_{UV,n} = Q_{UV,n-1} + \Delta t_n \overline{UV}_{G,n} \frac{A_r}{V_t}; \qquad \Delta t = t_n - t_{n-1} \tag{6}$$

where t_n (s) is the time corresponding to n-water sample, V_t the total reactor volume (1 L), A_r the illuminated surface area (0.0768 m^2) and $\overline{UV}_{G,n}$ the average solar ultraviolet radiation (W m^{-2}) measured during the period $\Delta t_n(s)$.

2.5. Procedure and analysis

One liter of MB solution with different initial concentrations (i.e. 10, 20, and 30 mg/L) containing 4 wt% TiO_2 embedded in the organic membrane was illuminated with solar light for 5 h. The pH of the solution was not adjusted (Free pH) and the temperature was not controlled; varying from 22 to 30 ℃.

One liter of MB solution was prepared with diverse pH (i.e. 3, 5, 7, 9, and 10) in order to study the effect of pH on MB photodegradation. A 2 mL sample was pipetted out at 10 min intervals and the change in transparency of the dye solution was observed. The dye concentration was recorded by a UV–visible spectrophotometer (Shimadzu-1800). The changes in the concentration of MB were monitored at their characteristic absorption wavelengths of 609 and 664 nm using the UV–visible spectrophotometer. The absorbance at 664 nm was employed to monitor the discoloration of MB. The influence of light source on the degradation efficiency was examined at constant dye concentration 10 mg/L using the organic membrane with 4 wt% catalyst.

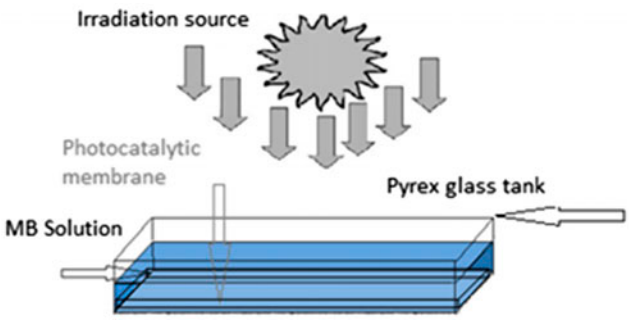

Fig. 2. Solar photoreactor.

2.6. Adsorption test

The adsorption experiments were performed with the dye solution at different concentrations. One liter of the aqueous dye solution was kept in contact with the TiO_2/PS composite membrane over 5 h. In order to avoid the photoreaction of TiO_2, the samples were kept in the dark for the entire period of the experiment. The concentration of the dye solution was determined from its absorbance at 664 nm. The amount of dye adsorbed on the catalyst was calculated by a mass balance. UV spectral analysis was carried out using UV–visible spectrophotometry.

3. Results and discussion

3.1. Membrane characterization

From Fig. 3(a), the surface characterization of the composite membrane PS/TiO_2 shows homogeneity and from Fig. 3(b) thickness was estimated to be around 30 μm as observed. The distribution of TiO_2 particles is relatively uniform in the matrix suggesting that the synthesized membranes are homogeneous in nature and hence form a dense membrane Fig. 3(c).

3.2. Photocatalyst physical properties and photodegradability of methylene blue

The Brunauer–Emmett–Teller (BET) surface area of $TiO_2$was found to be 4.61 m^2 g^{-1}. Measurement of X-ray diffraction indicated that TiO_2 has a structure consisting of 90% anatase and 10% rutile. The average particle size was found to be 48 nm.

Photocatalytic degradation of MB with commercial TiO_2 catalyst using the photocatalytic reactor at 300 min of UV irradiation indicated that 70% of the dye was degraded in the presence of TiO_2 incorporated in the membrane (Fig. 4). When the dye was UV irradiated without catalyst there was a low degradation (i.e. 35%). The same experiment when performed in the absence of UV light but with TiO_2, only a 3%

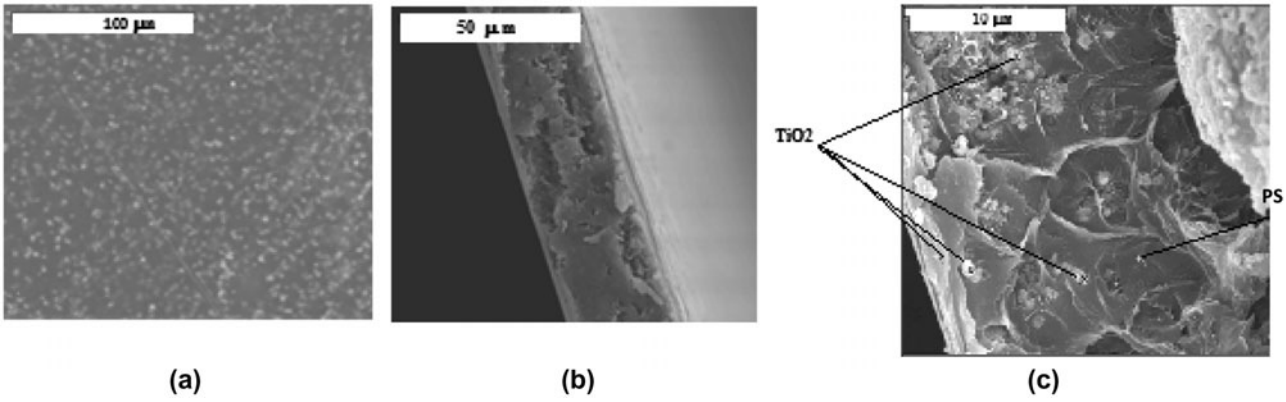

Fig. 3. SEM images of (a) surface, and (b,c) cross section of TiO_2/PS composite membrane at 500×, 1,000×, and 4,000× magnification, respectively.

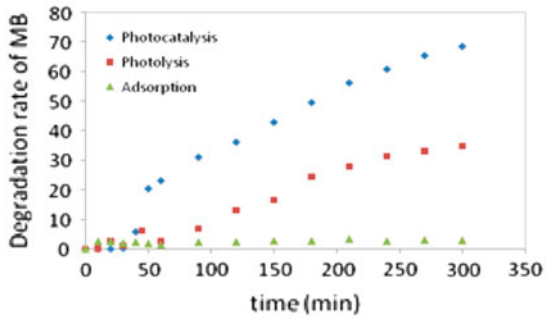

Fig. 4. Photodegradability of MB (V_t = 1 L; MB = 10 mg/L; pH 6–7; catalyst load 4 wt% in the casting solution).

decrease in dye concentration was observed. This was apparently due to adsorption of the dye on the surface of the catalyst.

The photocatalytic degradation of MB dye using TiO_2 obeyed pseudo-first-order kinetics. At low initial dye concentration, the rate expression is given by Eq. (2), where k_{app} is the pseudo-first-order rate constant. Integration of Eq. (2) (with the limit of $C = C_0$ at $t = 0$ with C_0 being the equilibrium concentration of the bulk solution) gives Eq. (3), where C_0 is the equilibrium concentration of dye and C is the concentration at time t.

3.3. Effect of initial dye concentration

The influence of the initial concentration of the dye solution on the photocatalytic degradation is an important aspect in determining the effectiveness of the process. The photodegradation rate decreased with increasing initial dye concentration which varied between 10 and 30 mg L^{-1} (Fig. 5). After 5 h, the highest level of decomposition was observed at C/C_o = 0.30 (i.e. 70% degradation) for C_o = 10 mg/L. A lower degree of decomposition at C/C_o = 0.54 (i.e. 46% degradation) was obtained for 20 mg/L, while for 30 mg/L dye, C/C_o only decreased to 0.70 at 5 h irradiation (i.e. 30% degradation of MB dye).

In Fig. 5 very similar curves were observed using solar light when the extent of degradation was represented vs. time. Even if degradation profiles were similar in these three cases, other parameters must be taken into account for better comparison. This is the accumulated energy (Fig. 6). An explanation for this behavior is that as the initial concentration increases, more and more organic substances are adsorbed on the surface of TiO_2; therefore, the generation of hydroxyl radicals will be reduced since there are fewer active sites for adsorption of hydroxyl ions and the generation of hydroxyl radicals. Furthermore, it can be argued that as the concentration of the dye solution increases, photons are intercepted before they can reach the catalyst surface. Hence the absorption of

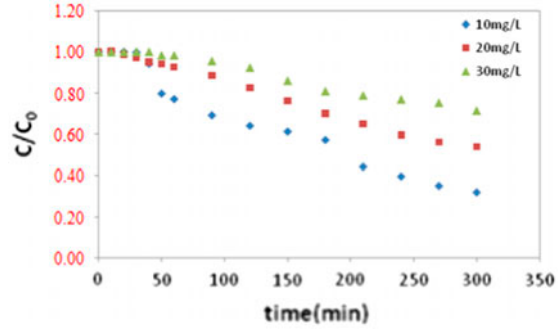

Fig. 5. Effect of MB initial concentration on photocatalytic degradation (V_t = 1 L, catalyst load 4 wt% in the casting solution, pH 6–7, sun light).

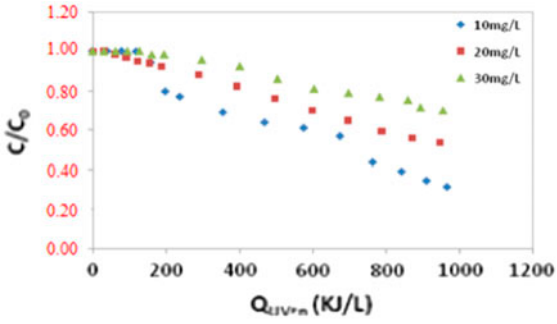

Fig. 6. Solar photocatalytic degradation of different initial MB concentrations vs. the quantity of accumulated energy. (V_t = 1 L, catalyst load 4 wt% in the casting solution, pH 6–7, sun light).

photons by the catalyst decreases, and consequently the degradation level (i.e. C/C_o) is reduced [44–47].

The UV–vis spectra of MB solutions (10 and 30 mg/L) at different irradiation times are shown in Figs. 7 and 8. There was no significant change in UV spectra during irradiation. The intensity at 609 and 664 nm decreased gradually during the degradation. This revealed that the intermediates do not absorb at the analytical wavelengths of 609 and 664 nm [47].

Fig. 7. The changes in UV–vis spectra of MB under sun light irradiation in the presence of PS/TiO_2 composite membrane during 300 min. (MB = 10 mg/L; pH 6–7; catalyst load 4 wt% in the casting solution; V_t = 1 L).

3.4. Effect of pH on the MB degradation

Fig. 9 shows the time-reduced concentration profiles of MB degradation at various pH. The extent of photocatalysis increased with increasing pH. At higher

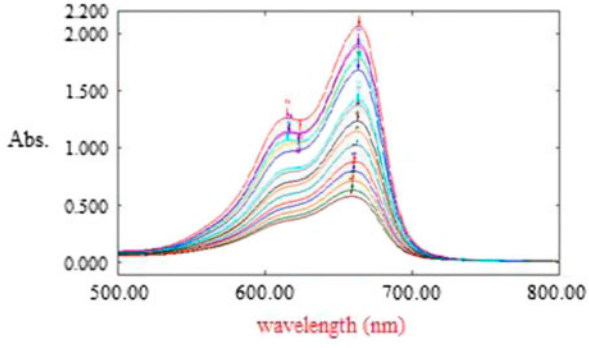

Fig. 7. The changes in UV–vis spectra of MB under sun light irradiation in the presence of PS/TiO_2 composite membrane during 300 min. (MB = 10 mg/L; pH 6–7; catalyst load 4 wt% in the casting solution; V_t = 1 L).

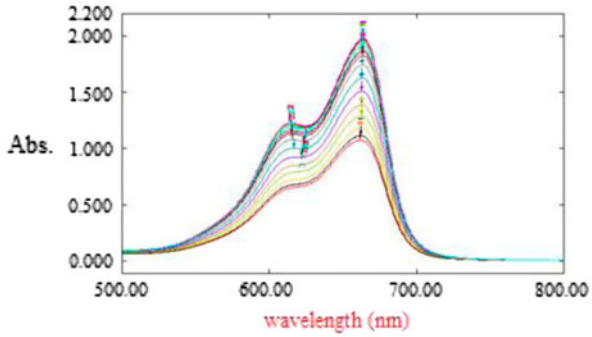

Fig. 8. The changes in UV–vis spectra of MB on under sun light irradiation and the presence of PS/TiO_2 composite membrane during 300 min. (MB = 30 mg/L; pH 6–7; catalyst load 4 wt% in the casting solution; V_t = 1 L).

pH (11), there was probably an excess of hydroxyl anions, which would have facilitated photogeneration of the hydroxyl radicals [48–50]. The interpretation of pH effects on the efficiency of dye photodegradation process is a very difficult task since it has multiple roles. Due to the amphoteric behavior of most semiconductor oxides, an important parameter governing the rate of reaction taking place on semiconductor particle surface is the pH, since it influences the surface charge properties of the photocatalysts. Furthermore, industrial effluents may not be neutral. Therefore, the effect of pH on the rate of degradation needs to be considered.

To introduce the influence of other parameters such as surface area, treated volume, and accumulated energy, Fig. 10 was plotted using Eq. (6). The resulting degradation profiles in Fig. 10 were similar to those vs. time (i.e. Fig. 9). The degradation rate for dye was found to be lower at lower pH values, which increased with an increase in reaction pH. The highest efficiency was observed at pH 11 in the presence of photocatalyst. This effect may be attributed to more

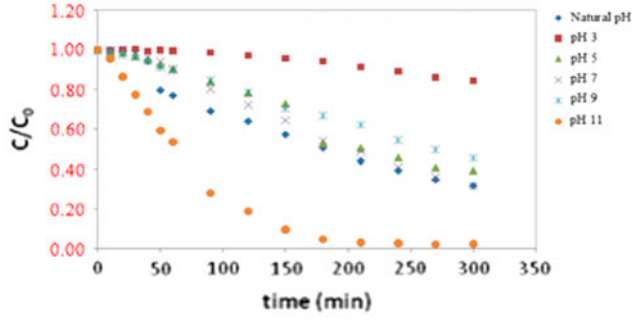

Fig. 9. Effect of initial pH on photocatalytic degradation of MB. UV Sun, catalyst load 4 wt% in the casting solution, $[MB]_0$ = 10 mg L^{-1}.

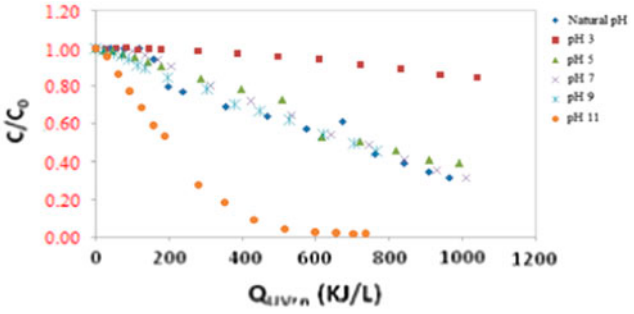

Fig. 10. Solar photocatalytic degradation of MB vs. the quantity of accumulated energy for different initial pHs. (V_t = 1 L, catalyst load 4 wt% in the casting solution, $[MB]_0$ = 10 mg L^{-1}, UV sun).

efficient generation of hydroxyl radicals by the photocatalyst with increasing concentration of OH^-. At alkaline pH values, the hydroxyl radicals have to diffuse away and degrade the dye in the bulk solution. Similar results have been reported by other research groups for acetate ion, acid blue 40, and chrysoidine Y(1) [51,52].

The shape of the curves in Fig. 9 is exponential decay, which predicts that the kinetics of degradation of MB is pseudo-first-order. Rate constants for each concentration were determined by linear regression from the plot of the evolution of -ln (C/C_0) function of time (Fig. 11). The initial rate of photodegradation was studied as a function of the initial concentration of the substrates using the linearized form of the Langmuir–Hinshelwood equation, which was well fitted by the membranes over the whole range of concentration, and from which the apparent rate constants k_{app}, initial rates degradation (r_0) and time of half reaction $t_{1/2}$ were evaluated and are summarized in Table 1.

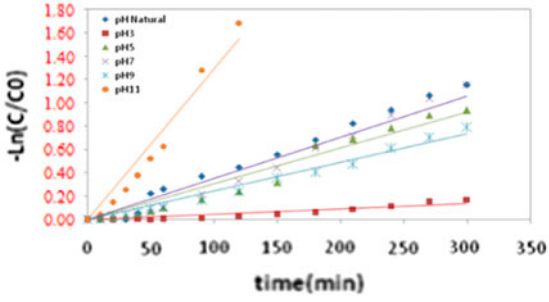

Fig. 11. Kinetics of MB degradation for different initial pHs. (V_t = 1 L, catalyst load 4 wt% in the casting solution, MB_0 = 10 mg L^{-1}, sun light).

Table 1
Values of kinetic constants, initial rates, degradation rate, and the time of half-reaction after 300 min of solar irradiation for different initial pH. (V_t = 1 L, catalyst load 4 wt% in the casting solution, $[MB]_0$ = 10 mg L^{-1}, sun light)

pH	k_{app} (min^{-1})	r_0 (mg/L min)	$t_{1/2}$ (min)	R%
3	0.0001	0.001	6,931	16
5	0.003	0.030	231	61
7	0.003	0.027	231	68
9	0.002	0.020	347	55
11	0.012	0.105	58	98

3.5. Effect of irradiation source

The influence of light source and intensity on the degradation efficiency has been examined at constant dye concentration (10 mg/L) and at 4 wt% casting solution. The results showed a large variation on MB removal with the change in light source. Fig. 12 presents the changes in dye concentration during the photocatalytic process using solar and UV Lamp irradiation.

Using the sun irradiation, the mean UV accumulated energy during this experimental day was Q_{UV} = 965 kJ/L, we obtained 68% of MB degradation or removal, after 300 min. In comparison with the UV lamp, there was only a 20% degradation or removal on MB. It is evident that the percentage of photodegradation increases with increasing light intensity as shown in Figs. 13 and 14.

UV irradiation generates the photons required for the electron transfer from the valence band to the conduction band of a semiconductor photocatalyst, and the energy of a photon is related to its wavelength, and the overall energy input to a photocatalytic process is dependent on light intensity. The rate of

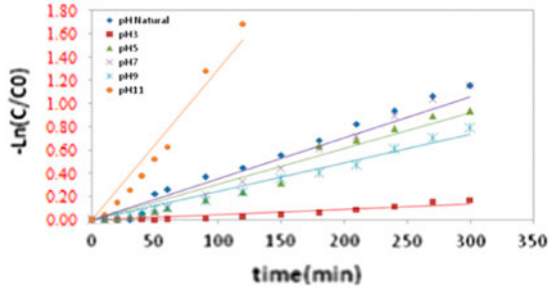

Fig. 12. Photolytic degradation of MB, normalized MB concentration vs. time. (V_t = 1 L, TiO_2 load 4 wt%, MB_0 = 10 mg L^{-1}, sun light and UV lamp). Changes in dye concentration during the photocatalytic process using solar and UV Lamp irradiation (2 Phillips PL-L 24 W/10/4P lamps (λ_{max} = 365 nm)).

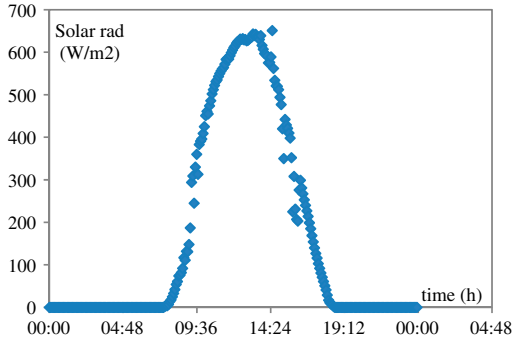

Fig. 13. Time evolution of the solar flux for an experimental day.

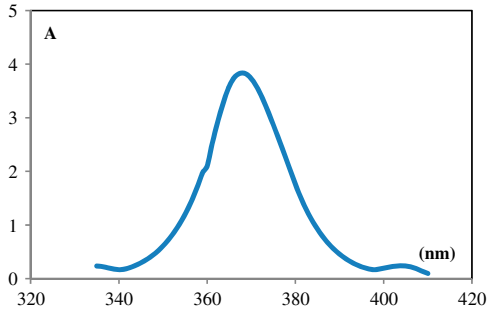

Fig. 14. Spectral distribution of the lamp. Philips PL-L 24 W/10/4P.

degradation increases when more radiation falls on the catalyst surface and hence more hydroxyl radicals are produced [13,47,53].

4. Conclusions

It has been demonstrated that flat organic photocatalytic membranes can be fabricated and employed for the efficient degradation of MB organic dye in aqueous solution. The MB dye was successfully degraded by TiO_2 fixed on PS membranes in aqueous solution under irradiation by solar light. The dye was resistant to direct photolysis especially at high concentrations. The photocatalytic degradation obeys pseudo-first-order kinetics at low initial concentration. The optimum pH for efficient removal of dye was found to be 11. An increase in initial dye concentration decreases the degradation rate. The applicability of Langmuir–Hinshelwood kinetic equation revealed that the degradation of MB occurs mainly on the surface of the photocatalyst. The concept and results provide a promising platform for fabricating highly efficient organic photocatalytic membranes for water treatment.

References

[1] M.A. Shannon, P.W. Bohn, M. Elimelech, J.G. Georgiadis, B.J. Mari˜nas, A.M. Mayes, Science and technology for water purification in the coming decades, Nature 452 (2008) 301–310.
[2] K. Xuebin, S. Ribbens, F. Yiqun, H. Liu, P. Cool, D. Yang, H. Zhua, Integrating efficient filtration and visible-light photocatalysis by loading Ag-doped zeolite Y particles on filtration membrane of alumina nanofibers, J. Membr. Sci. 375 (2011) 69–74.
[3] M.N. Chong, B. Jin, C.W.K. Chow, C. Saint, Recent developments in photocatalytic water treatment technology: A review, Water Res. 44 (2010) 2997–3027.
[4] S. Ahmed, M.G. Rasul, W.N. Martens, R. Brown, M.A. Hashib, Heterogeneous photocatalytic degradation of phenols in wastewater: A review on current status and developments, Desalination 261 (2010) 3–18.
[5] W.A. Zeltner, D.T. Tompkins, Shedding light on photocatalysis, in: American society of heating, refrigerating and air-conditioning, Engineers 6 (2005), p. 111.
[6] P. Cui, X. Zhao, M. Zhou, L. Wang, Photocatalysis-membrane separation coupling reactor and its application, Chin. J Catal. 27(9) (2006) 752–754.
[7] A.A. Habibpanah, S. Pourhashem, H. Sarpoolaky, Preparation and characterization of photocatalytic titania–alumina composite membranes by sol–gel methods, J. Eur. Ceram. Soc. 31 (2011) 2867–2875.
[8] D. Li, H. Haneda, S. Hishita, N. Ohashi, Visible-light-driven N−F−codoped TiO_2 photocatalysts. 2. Optical characterization, photocatalysis, and potential application to air purification, Chem. Mater. 17 (2005) 2596–2602.
[9] P. Pichat, J. Disdier, C. Hoang-Van, D. Mas, G. Goutailler, C. Gaysse, Purification/deodorization of indoor air and gaseous effluents by TiO_2 photocatalysis, Catal. Today 63 (2000) 363–369.
[10] X.Z. Li, F.B. Li, Study of Au/Au3+ -TiO_2 photocatalysts toward visible photooxidation for water and wastewater treatment, Environ. Sci. Technol. 35 (2001) 2381–2387.
[11] A. Haarstrick, O.M. Kut, E. Heinzle, TiO_2-assisted degradation of environmentally relevant organic compounds in wastewater using a novel fluidized bed photoreactor, Environ. Sci. Technol. 30 (1996) 817–824.
[12] J.C. Yu, J.G. Yu, J.C. Zhao, Enhanced photocatalytic activity of mesoporous and ordinary TiO_2 thin films by sulfuric acid treatment, Appl. Catal., B 36 (2002) 31–43.
[13] I.K. Konstantinou, T.A. Albanis, TiO_2-assisted photocatalytic degradation of azo dyes in aqueous solution: Kinetic and mechanistic investigations, Appl. Catal., B 49 (2004) 1–14.
[14] X.X. Yang, C.D. Cao, L. Erickson, K. Hohn, R. Maghirang, K. Klabunde, Photo-catalytic degradation of Rhodamine B on C-, S-, N-, and Fe-doped TiO_2 under visible-light irradiation, Appl. Catal. B Environ. 91 (2009) 657–662.
[15] J. Yang, J. Dai, C.C. Chen, J.C. Zhao, Effects of hydroxyl radicals and oxygen species on the 4-chlorophenol degradation by photoelectrocatalytic reactions with TiO_2-film electrodes, J. Photochem. Photobiol., A 208 (2009) 66–77.

[16] R. Vinu, G. Madras, Kinetics of sonophotocatalytic degradation of anionic dyes with nano-TiO_2, Environ. Sci. Technol. 43 (2009) 473–479.
[17] R. Scotti, M. D'Arienzo, F. Morazzoni, I.R. Bellobono, Immobilization of hydrothermally produced TiO_2 with different phase composition for photocatalytic degradation of phenol, Appl. Catal., B 88 (2009) 323–330.
[18] T.A. McMurray, J.A. Byrne, P.S.M. Dunlop, J.G.M. Winkelman, B.R. Eggins, E.T. McAdams, Intrinsic kinetics of photocatalytic oxidation of formic and oxalic acid on immobilised TiO_2 films, Appl. Catal., A 262 (2004) 105–110.
[19] S. Kagaya, K. Shimizu, R. Arai, K. Hasegawa, Separation of titanium dioxide photocatalyst in its aqueous suspensions by coagulation with basic aluminium chloride, Water Res. 33 (1999) 1753–1755.
[20] X.D. Xue, J.F. Fu, W.F. Zhu, X.C. Guo, Separation of ultrafine TiO_2 from aqueous suspension and its reuse using cross-flow ultrafiltration (CFU), Desalination 225 (2008) 29–40.
[21] P. Lei, F. Wang, X. Gao, Y. Ding, S. Zhang, J. Zhao, S. Liu, M. Yang, Immobilization of TiO_2 nanoparticles in polymeric substrates by chemical bonding for multicycle photodegradation of organic pollutants, J. Hazard. Mater. 227–228 (2012) 185–194.
[22] A. Fernandez, G. Lassaletta, V.M. Jimenez, A. Justo, A.R. Gonzalez-Elipe, J.-M. Herrmann, H. Tahiri, Y. Ait-Ichou, Preparation and characterization of TiO_2 photocatalysts supported on various rigid supports (glass, quartz and stainless steel). Comparative studies of photocatalytic activity in water purification, Appl. Catal., B 7 (1995) 49–63.
[23] S. Gelover, P. Mondragón, A. Jiménez, Titanium dioxide sol-gel deposited over glass and its application as a photocatalyst for water decontamination, J. Photochem. Photobiol. A 165 (2004) 241–246.
[24] N. Kieda, T. Tokuhisa, Immobilization of TiO_2 photocatalyst particles on stainless steel substrates by electrolytically deposited Pd and Cu, J. Ceram. Soc. Jpn. 114 (2006) 42–45.
[25] S.H. Yao, J.Y. Liand, Z.L. Shi, Immobilization of TiO_2 nanoparticles on activated carbon fiber and its photodegradation performance for organic pollutants, Particuology 8 (2010) 272–278.
[26] H.C. Liang, X.Z. Li, Visible-induced photocatalytic reactivity of polymer–sensitized titania nanotube films, Appl. Catal. B 86 (2009) 8–17.
[27] J.I. Lim, B. Yu, K.M. Woo, Y.K. Lee, Immobilization of TiO_2 nanofibers on titanium plates for implant applications, Appl. Surf. Sci. 255 (2008) 2456–2460.
[28] J. Zeng, S.L. Liu, J. Cai, L. Zhang, TiO_2 immobilized in cellulose matrix for photocatalytic degradation of phenol under weak UV light irradiation, J. Phys. Chem. C 114 (2010) 7806–7811.
[29] S. Matsuzawa, C. Maneerat, Y. Hayata, T. Hirakawa, N. Negishi, T. Sano, Immobilization of TiO_2 nanoparticles on polymeric substrates by using electrostatic interaction in the aqueous phase, Appl. Catal., B 83 (2008) 39–45.
[30] K. Li, Ceramic membranes for separation and reaction. John Wiley & Sons, England, 2007.
[31] H. Zhang, X. Quan, S. Chen, H. Zhao, Y. Zhao, Fabrication of photocatalytic membrane and evaluation its efficiency in removal of organic pollutants from water, Sep. Purif. Technol. 50 (2006) 147–155.
[32] R. Molinari, M. Mungari, E. Drioli, A. Di Paola, V. Loddo, L. Palmisano, M. Schiavello, Study on a photocatalytic membrane reactor for water purification, Catal. Today 55 (2000) 71–78.
[33] A. Alem, H. Sarpoolaky, M. Keshmiri, Sol–gel preparation of titania multilayer membrane for photocatalytic applications, Ceram. Int. 35 (2009) 1837–1843.
[34] R. Molinari, L. Palmisano, E. Drioli, M. Schiavello, Studies on various reactor configurations for coupling photocatalysis and membrane processes in water purification, J. Membr. Sci. 206 (2002) 399–415.
[35] S. Mozia, Photocatalytic membrane reactors (PMRs) in water and wastewater treatment. A review, Sep. Purif. Technol. 73 (2010) 71–91.
[36] S.S. Chin, K. Chiang, A.G. Fane, The stability of polymeric membranes in a TiO_2 photocatalysis process, J. Membr. Sci. 275 (2006) 202–211.
[37] S.H. Kim, S.-Y. Kwak, B.-H. Sohn, T.H. Park, Design of TiO_2 nanoparticle self-assembled aromatic polyamide thin-film-composite (TFC) membrane as an approach to solve biofouling problem, J. Membr. Sci. 211 (2003) 157–165.
[38] C.S. Turchi, D.F. Ollis, Photocatalytic degradation of organic water contaminants: Mechanisms involving hydroxyl radical attack, J. Catal. 122 (1990) 178–192.
[39] W.Z. Tang, An. Huren An, UV/TiO_2 photocatalytic oxidation of commercial dyes in aqueous solutions, Chemosphere 31(9) (1995) 4157–4170.
[40] S. Chakrabarti, B.K. Dutta. Photocatalytic degradation of model textile dyes in wastewater using ZnO as semiconductor catalyst. J. Hazard. Mater., B 112 (2004) 269–278.
[41] S. Malato, J. Blanco, C. Richter, B. Milow, M.I. Maldonado, Solar photocatalytic mineralization of commercial pesticides: Methamidophos, Chemosphere 38 (1999) 1145–1156.
[42] N. De la Cruz, R.F. Dantas, J. Giménez, S. Esplugas, Photolysis and TiO_2 photocatalysis of the pharmaceutical propranolol: Solar and artificial light, Appl. Catal., B Environ. (2013) 249–256.
[43] H.O.S. João, J.P. VilarVitor, T. Borges Maria, O. González, S. Esplugas, A.R. RuiBoaventura, Photocatalytic degradation of oxytetracycline using TiO_2 under natural and simulated solar radiation, Solar Energy 85 (2011) 2732–2740.
[44] B. Krishnakumar, M. Swaminathan, Influence of operational parameters on photocatalytic degradation of a genotoxic azo dye Acid Violet 7 in aqueous ZnO suspensions, Spectrochim. Acta, Part A 81 (2011) 739–744.
[45] M. Muneer, R. Philip, S. Das, Photocatalytic degradation of waste water pollutants. Titanium dioxidemediated oxidation of a textile dye, Acid Blue 40, Res. Chem. Intermed. 23 (1997) 233–246.
[46] S. Ruan, F. Wu, T. Zhang, W. Gao, B. Xu, M. Zhao, Surface-state studies of TiO_2 nanoparticles and photocatalytic degradation of methyl orange in aqueous TiO_2dispersionsMater, Chem. Phys. 69 (2001) 7–9.
[47] M.A. Behnajady, N. Modirshahla, R. Hamzavi, Kinetic study on photocatalytic degradation of C.I. Acid Yellow 23 by ZnO photocatalyst, J. Hazard. Mater., B 133 (2006) 226–232.

[48] H. Zhao, S. Xu, J. Zhong, X. Bao, Kinetic study on the photo-catalytic degradation of pyridine in TiO_2 suspension systems, Catal. Today 93-95 (2004) 857–861.
[49] M. Bekbolet, I. Balcioglu, Photocatalytic degradation kinetics of humic acid in aqueous tio dispersions: The influence of hydrogen peroxide and bicarbonate ion, Water Sci. Technol. 34 (1996) 73–80.
[50] M.S.T. Goncalves, E.M.S. Pinto, P. Nkeonye, A.M.F. Oliveiracampos, Degradation of and its simulated dyebath wastewater by heterogeneous photocatalysis, Dyes and Pigm. 64 (2005) 135–139.
[51] T. Takagishi, N. Katsuda, Photodegradation of dyes by spectro-irradiation, in: Int. Conf. Exhib. AACTT, 1999, pp. 358–366.
[52] C. Koval, Proceedings of the Symposium on Photoelectrochemistry, The Electrochemical Society, Pennington NJ, 124 (1991) 478–491.
[53] N. Daneshvar, M. Rabbani, N. Modirshahla, M.A. Behnajady, Kinetic modeling of photocatalytic degradation of Acid Red 27 in UV/TiO_2 process, J. Photochem. Photobiol., A 168 (2004) 39–45.